Resonance Poles in a Simple Model of S-Wave Pseudoscalar-Meson–Baryon Scattering*

R. K. LOGAN AND H. W. WYLD, JR.
Department of Physics, University of Illinois, Urbana, Illinois
(Received 6 February 1967)

In an earlier work a numerical calculation was made of S-wave pseudoscalar-meson–baryon scattering in a simple broken-$SU(3)$ model based on a static vector-meson exchange potential and coupled-channel Schrödinger equations. In the present work these calculations are extended to finding the location of the poles of the scattering matrix in the multisheeted complex energy plane and finding the motion of these poles as the strength of the potential is varied. Particular attention is paid to the behavior of the poles when the potential strength is such that there is a resonance closed to a threshold.

I. INTRODUCTION

In a recent paper[1] one of us (H.W.W.) reported some numerical calculations of S-wave pseudoscalar-meson–baryon scattering in a simple model with broken-SU(3) symmetry. In this model the interaction between the pseudoscalar mesons and the baryons is approximated by a static vector-meson-exchange potential and the dynamics is approximated by coupled-channel Schrödinger equations, which are solved exactly on a computer. Several virtual bound-state S-wave resonances were found in these calculations. There is an $I=0$, $Y=0$ resonance which can be identified with the $Y_0^*(1405)$ and which has also been discussed by Dalitz, Rjasekaran, and Wong.[2] In addition we found, for an appropriate choice of the coupling constant, an $I=\frac{1}{2}$, $Y=1$ resonance which we identified with $N_{1/2}^*(1570)$, an $I=0$, $Y=0$ resonance which can be perhaps identified with $Y_0^*(1670)$, and an $I=\frac{1}{2}$, $Y=-1$ resonance which has not been observed as yet. There was no evidence of resonance behavior in the $I=1$, $Y=0$ state.

These numerical calculations were carried through for real physical energies. The eigenphases, i.e., the multichannel generalization of phase shifts, were calculated and resonances were associated with the rapid increase of an eigenphase through 90°. While this is certainly the most efficient way of doing the numerical calculation and yields all quantities which could conceivably be measured experimentally, it does not give directly very much information about the analytic structure of the scattering matrix in the complex-energy plane. In particular a resonance is associated with one or more poles of the scattering matrix in the complex-energy plane and in order to "understand" the resonance it is desirable to locate these poles and see how they move when the coupling constant is varied. While this would in general be simple if an analytic formula were available for the scattering matrix, for a numerical example such as the model discussed above, it requires a separate investigation. In this paper we report the results of the numerical calculation of the location of the resonance poles for the above model.

This model is described by coupled-channel Schrödinger equations

$$-\frac{1}{2\mu_i(E)}\frac{d^2U_i(r)}{dr^2}+\sum_j V_{ij}(r)U_j(r)=(E-m_{1i}-m_{2i})U_i(r). \quad (1)$$

The matrix potential is of the form

$$V_{ij}(r)=-\frac{G^2}{4\pi}\frac{e^{-m_v r}}{r}C_{ij}, \quad (2)$$

where C_{ij} is a numerical matrix of SU(3) crossing coefficients, the details of which are given in Ref. 1. The energy-dependent reduced mass,

$$\mu_i(E)=[E^2-(m_{1i}-m_{2i})^2][E+m_{1i}+m_{2i}]/8E^2, \quad (3)$$

is defined in such a way that the relation between energy E and momentum p_i in the ith channel,

$$E=m_{1i}+m_{2i}+p_i^2/2\mu_i(E), \quad (4)$$

is an exact relation for relativistic kinematics.

As is well known the asymptotic solution of a scattering problem involves an ingoing wave of unit amplitude and an outgoing wave whose amplitude is given by the scattering matrix S_{ji}:

$$\delta_{ji}e^{-ip_ir}-S_{ji}e^{ip_jr}. \quad (5)$$

At a pole of the scattering matrix, the Schrödinger equation has a solution with an asymptotic form which is pure outgoing wave. Thus at a pole of the scattering matrix at some complex energy E, the radial wave function $U_i(r)$ of Eq. (1) satisfies the boundary conditions

$$\begin{aligned} U_i(r)&\to 0, & r&\to 0,\\ U_i(r)&\to K_ie^{ip_ir}, & r&\to\infty. \end{aligned} \quad (6)$$

The coupled equations (1) together with the boundary conditions (6) provide a well-defined eigenvalue problem for a complex eigenvalue E. We can restate the eigenvalue problem in an equivalent way as follows: If

* This work was supported by the U. S. Office of Naval Research under Contract Task A-05-T and by the National Science Foundation under Grant No. NSF GP 6198.
[1] H. W. Wyld, Jr., Phys. Rev. 155, 1649 (1967).
[2] R. H. Dalitz, T .C. Wong, G. Rajasekaran, Phys. Rev. 153, 1617 (1967).

there are N channels we can find N solutions of the coupled equations (1) which vanish at $r=0$ and have unit derivative in one channel at $r=0$. We call these solutions $u_{ij}(r)$, where the first index i indicates the channel and the second index j the number of the solution. Thus the boundary conditions on these N solutions $u_{ij}(r)$ are

$$u_{ij}(0)=0,\quad u_{ij}'(0)=\delta_{ij}. \tag{7}$$

We can find another set of N solutions of Eqs. (1) which reduce to an outgoing wave in one channel outside the range of the potential. We call these solutions $v_{ij}(r)$ and they satisfy the boundary conditions

$$v_{ij}(r)=\delta_{ij}e^{ip_ir},\quad r\to\infty,\qquad v_{ij}'(r)=\delta_{ij}ip_ie^{ip_ir},\quad r\to\infty. \tag{8}$$

If E is an eigenvalue of the complex-eigenvalue problem defined by Eqs. (1) and (6), it is possible to find an appropriate linear combination

$$\sum_j u_{ij}(r)A_j=U_i(r) \tag{9}$$

of the solutions (7) which will match a different linear combination

$$\sum_j v_{ij}(r)B_j=U_i(r) \tag{10}$$

of the solutions (8). In this way we will have a solution which satisfies both boundary conditions (6). In practice we match wave functions and derivatives at a point $r=a$:

$$\sum_j (u_{ij}(a)A_j-v_{ij}(a)B_j)=0,\qquad \sum_j (u_{ij}'(a)A_j-v_{ij}'(a)B_j)=0. \tag{11}$$

This gives the $2N\times 2N$ determinantal condition:

$$D=\det\begin{pmatrix} u(a) & -v(a) \\ u'(a) & -v'(a)\end{pmatrix}=0. \tag{12}$$

The numerical calculation proceeds along the following lines, suggested to us by D. G. Ravenhall. The solutions $u_{ij}(r)$ and $v_{ij}(r)$ are found for two assumed complex energies E_1 and E_2, and the determinant in Eq. (12) is evaluated for each energy. Since the assumed energies will not in general be eigenvalues the determinants will not vanish, so we have two nonvanishing determinants D_1 and D_2. We assume the determinant can be expanded in a Taylor series in the energy near the true eigenvalue E. Then keeping only one term in the expansion we have

$$D_1\simeq C(E-E_1),\qquad D_2\simeq C(E-E_2). \tag{13}$$

Eliminating C we find an estimate of E:

$$E\simeq E_2\left(1-\frac{D_2}{D_1}\frac{E_1}{E_2}\right)\Big/\left(1-\frac{D_2}{D_1}\right). \tag{14}$$

This procedure is now iterated, i.e., we start with E_2 and E in place of E_1, E_2 and calculate an improved estimate of E, *etc.* The iteration converges rapidly if one starts anywhere near the correct eigenvalue.

We now remind the reader of the multisheeted character of the complex-energy plane for a multichannel scattering problem. The scattering matrix for a given angular-momentum state is a real analytic function of the energy E with a unitarity cut starting at each threshold. The branch point at each threshold is of square-root type, corresponding to the two momenta ($\pm p_i$) which yield the same energy in a given channel—see Eqs. (4) and (5). Thus for an N channel problem the complex-energy plane has 2^N sheets. The best way to specify a sheet is to give the sign of the imaginary part of the momenta in each channel. We shall use a symbol such as $---+$ for a four-channel problem. This means that the sign of the imaginary part of the momentum is negative in the first three channels and positive in the fourth channel. Naturally, the channels are listed in order of increasing mass. For the case of 2 channels (or 2 neighboring channels in a symbol such as $---+$) the four sheets are often labelled: Sheet I$=++$, Sheet II$=-+$, Sheet III$=--$, Sheet IV$=+-$. The physical sheet is, of course, $++++$. On this sheet the outgoing wave in the asymptotic wave function (5) is really an outgoing wave for the open channels and a decaying exponential for the closed channels. If we cross through the cut at some energy E, we will reverse the sign of the imaginary part of the momenta in all channels whose threshold is below E. Thus if we start on the physical sheet $++++$ and cross between the thresholds of channels 2 and 3 we go onto the neighboring unphysical sheet $--++$. If we now increase the energy above the threshold of channel 3 and then go back across the cut we find ourselves on a super unphysical sheet $++-+$.

Finally we note that it follows trivially from the form of Eqs. (1) and (6) that poles of the scattering matrix lie at complex-conjugate points on the same sheet. In the figures in the next section we show only one of this complex-conjugate pair of poles.

The behavior of the poles associated with a resonance, when parameters such as the coupling constant are varied so that the resonance crosses a threshold, has been discussed by several authors.[3] If the resonance is

[3] M. Ross, Phys. Rev. Letters **11**, 450 (1963); R. J. Eden and J. R. Taylor, *ibid.* **11**, 516 (1963); M. Nauenberg and J. C. Nearing, *ibid.* **12**, 63 (1964); R. H. Dalitz and G. Rajasekaran, Phys. Letters **5**, 373 (1963); G. Rajasekaran, Nuovo Cimento **31**, 697 (1964); C. R. Hagen, Phys. Rev. Letters **12**, 153 (1964); D. Amati, Phys. Letters **7**, 290 (1963); K. C. Wali and R. L. Warnock, Phys. Rev. **135**, B1358 (1964).

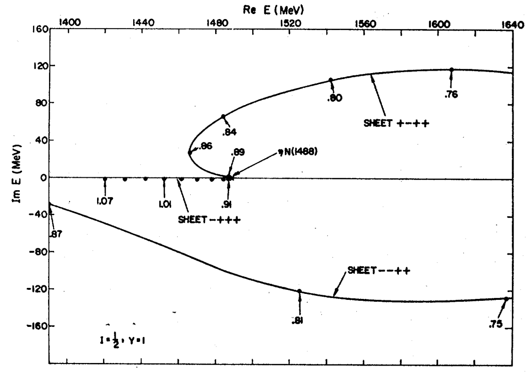

FIG. 1. Location of the poles of the S matrix in the complex-energy plane as a function of the coupling constant for the state $I=\frac{1}{2}$, $Y=1$. The numbers on the curves are values of the coupling constant $G^2/4\pi$ [see Eq. (2)]. For this state the threshold energies in MeV are $\pi N(1077)$, $\eta N(1488)$, $K\Lambda(1611)$, and $K\Sigma(1689)$.

far from threshold it is "caused" by a pole on the neighboring unphysical sheet. For example, if the resonance is between the second and third thresholds there is a pole on sheet $--++$; if the resonance is between the first and second thresholds there is a pole on sheet $-+++$. If the parameters of the problem are adjusted so that the resonance lies close to the second threshold, then the resonance is associated with both the poles on sheets $--++$ and $-+++$. In the numerical examples discussed below we shall see several examples of this effect.

II. NUMERICAL RESULTS

A. $I=\frac{1}{2}$, $Y=1$ State

For values of the coupling constant of physical interest there is a resonance close to the ηN threshold at 1488 MeV. Correspondingly there are poles on two adjacent unphysical sheets. The motion of these poles as the coupling constant is varied as shown in Fig. 1. The behavior of one of these poles is somewhat pathological. For values of the coupling constant larger than 0.91 this pole is on sheet $-+++$ just slightly (about 1 MeV) below the real axis. Thus for these values of the coupling constant we would have an extremely narrow resonance below the ηN threshold. For smaller values of the coupling constant the pole crosses the cut onto the adjacent unphysical sheet $+-++$ and rapidly moves away from the physical region in the peculiar fashion indicated in Fig. 1. There are no poles close to the physical region for energies substantially above the ηN threshold; consequently, the resonance rapidly disappears as the coupling constant is decreased so that the resonance energy moves above threshold. These results are in agreement with and serve to "explain" the corresponding results in Ref. 1.

In addition to the poles indicated in Fig. 1 we found a third pole on sheet $--++$. With increasing values of the coupling constant this pole moves nearly parallel to the imaginary energy axis, approaching the real axis at 1060 MeV. This pole is very far from the physical region.

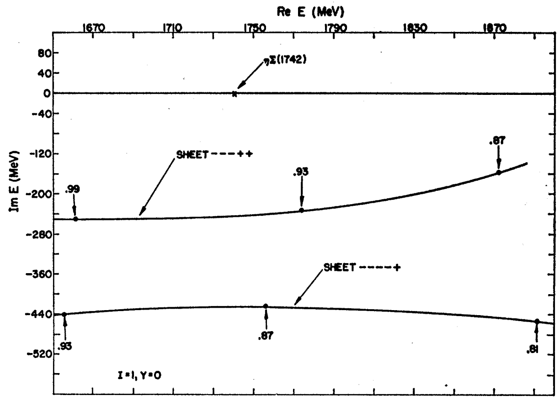

FIG. 2. Location of the poles of the S matrix in the complex-energy plane as a function of the coupling constant for the state $I=1$, $Y=0$. The numbers on the curves are values of the coupling constant $G^2/4\pi$ [see Eq. (2)]. For this state the threshold energies in MeV are $\pi\Lambda(1253)$, $\pi\Sigma(1331)$, $\bar{K}N(1435)$, $\eta\Sigma(1742)$, and $K\Xi(1814)$.

B. $I=1$, $Y=0$ State

For this five-channel problem there are poles on the neighboring unphysical sheets $---++$ and $----+$ close to the $\eta\Sigma$ threshold. As one can see from Fig. 2, they are so far from the real axis that they do not give rise to a real physical resonance. In the corresponding calculation in Ref. 1, one of the eigenphases goes through 90° extremely slowly.

C. $I=\frac{1}{2}$, $Y=-1$ State

For this state the motion of the poles shown in Fig. 3 is more or less normal. For values of the coupling constant larger than 0.90 the pole on sheet $-+++$ gives rise to a very narrow resonance below the $\Lambda\bar{K}$ threshold. For values of the coupling constant smaller

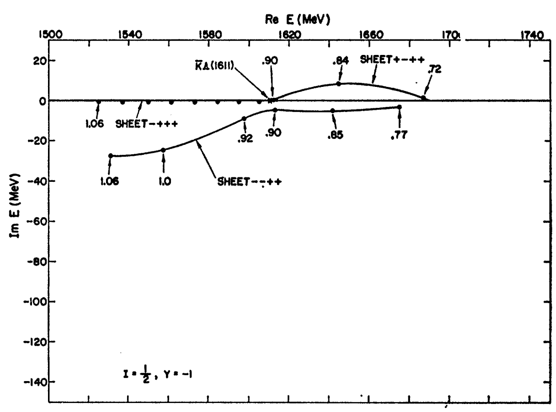

FIG. 3. Location of the poles of the S matrix in the complex-energy plane as a function of the coupling constant for the state $I=\frac{1}{2}$, $Y=-1$. The numbers on the curves are values of the coupling constant $G^2/4\pi$ [see Eq. (2)]. For this state the threshold energies in MeV are $\pi\Xi(1456)$, $\bar{K}\Lambda(1611)$, $\bar{K}\Sigma(1689)$, and $\eta\Xi(1867)$.

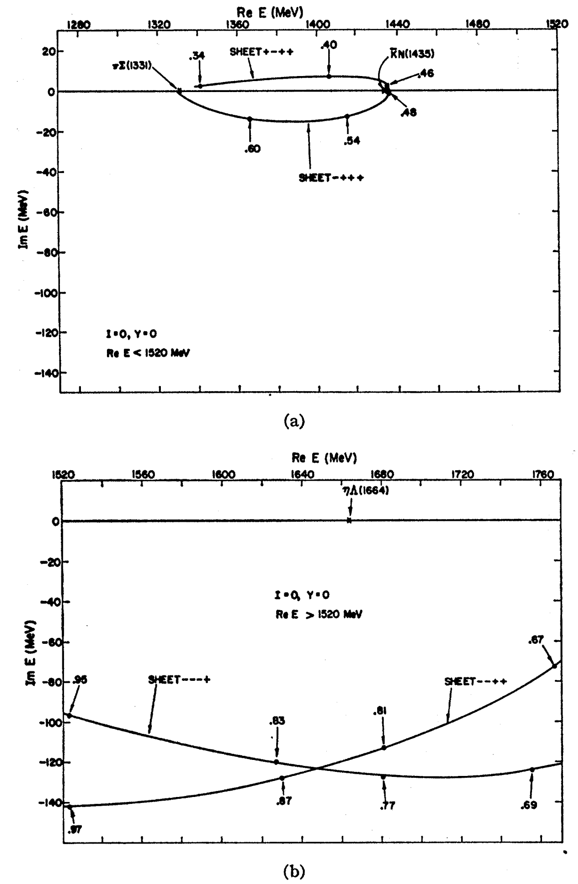

FIG. 4. Location of the poles of the S matrix in the complex-energy plane as a function of the coupling constant for the state $I=0$, $Y=0$. The numbers on the curves are values of the coupling constant $G^2/4\pi$ [see Eq. (2)]. For this state the threshold energies are $\pi\Sigma(1331)$, $\bar{K}N(1435)$, $\eta\Lambda(1664)$, and $K\Xi(1814)$. Figure 4(a) for Re$E<1520$ MeV shows the pole responsible for the $Y_0^*(1405)$ resonance. Figure 4(b) for Re$E>1520$ MeV shows the poles which are perhaps associated with the $Y_0^*(1670)$ resonance.

than 0.90 the pole on sheet $--++$ gives rise to a resonance of width $\sim$10 MeV above the $\Lambda\bar{K}$ threshold.

D. $I=0$, Y=0 State

For this state there are two resonances to consider. The motion of the corresponding poles is shown in Figs. 4(a) and 4(b). For a coupling constant of 0.56 there is a pole on sheet $-+++$ at an energy of 1400 MeV and a width of 30 MeV. This pole is to be associated with the $Y_0^*(1405)$ state. Note that as the coupling constant is decreased this pole moves above the $\bar{K}N$ threshold, crosses the cut onto sheet $+-++$ and then moves to lower energies. In addition there are poles on sheets $--++$ and $---+$ which, for somewhat larger values of the coupling constant, give rise to a very broad resonance near the $\eta\Lambda$ threshold. Again these results are in agreement with those of Ref. 1.

Finally we note the characteristic difference between the pole shown in Fig. 4(a) and the pairs of poles shown in Figs. 1, 2, 3, or 4(b). For the situation shown in Fig. 4(a) there is only one pole (not counting the complex-conjugate pole which is not shown). This pole is a virtual bound state in the $\bar{K}N$ channel and does not depend in any important way on the higher-mass coupled channels $\eta\Lambda$ and $K\Xi$. In fact we repeated the numerical calculation with the $\eta\Lambda$ and $K\Xi$ channels removed and obtained a diagram very similar to Fig. 4(a). There is no second pole on sheet $--++$ giving rise to a resonance above the $\bar{K}N$ threshold because there can be no virtual bound state in the $\bar{K}N$ system above threshold. For the other cases, Figs. 1, 3, 4(b), we have a virtual bound state in a higher-mass coupled channel, $K\Sigma$ for Fig. 1, $\bar{K}\Sigma$ for Fig. 3, and $K\Xi$ for Fig. 4(b). This virtual bound state is associated with two poles in the neighborhood of some lower threshold.